TRANSIENT HEAT TRANSMISSION THROUGH
CONCRETE FLOORS UNDER TOBACCO
CURING STRUCTURES

BY

ANDREW H. ADSIT

UNIVERSITY OF GEORGIA
AGRICULTURAL ENGINEERING DEPARTMENT
ATHENS, GA 30602

ADVISOR: DR. JOHN S. CUNDIFF

ANDREW H. ADSIT

DR. HARVEY B. MANBECK
CLUB ADVISOR

MARCH 26, 1979

INTRODUCTION

In 1978, Georgia produced 57.6 million kg of tobacco on 24.7 thousand hectares. Approximately 70% was cured in more than 9,000 bulk curing barns.

Mobile style bulk curing barns are presently manufactured as complete units much like mobile homes. At the farm site, they are placed on concrete slabs, installed with fuel and electric power and are ready for operation. Two basic designs are available. The down-draft barn and the updraft barn (See Fig. 1). In the down-draft barn, the fornance delivers heated air into the attic space or top plenum. It passes down the tobacco and is returned to the furnace in a bottom plenum formed by the barn floor and the concrete slab. In the updraft barn, the flow is reversed from the bottom plenum to the top plenum.

In current practice, the concrete slab is not insulated. The time integral temperature difference between the airstream in the bottom plenum and ambient soil is relatively high (3500 - 4000 C h for a six day cure). It is desirable then to measure the reduction in heat loss which can be achieved through the use of insulation under the concrete slab.

In the past little attention was paid to energy conservation in tobacco curing. Today, however, energy is a major cost factor. Some equipment manufacturers are insulating the mobile style units, and recommend that the concrete slab be insulated. However, the preparation of the foundation slab is the responsibility of the farmer, and there is need for research to determine the return on investment he can expect from insulation used under the concrete.

Chang et. al. (1978) measured the temperature in the soil under an existing bulk barn with 2.5 cm of polyurethane insulation board (R =1.1) on top of the concrete. By adjusting assumed soil moisture percentages he reduced the sum of squares between the measured temperatures and those calculated with finite difference techniques. His calculated heat loss was 45.6 MJ/m^2/cure with insulation, and 9.7 MJ/m^2/cure with insulation.

Cundiff and Sumner (1978) measured the temperature difference between the curing environment and ambient air during a six day cure in a factory insulated up-draft barn. They calculated heat loss through the roof and side walls using the composite thermal resistance for each surface and found total losses to be equivalent to 39.1 MJ/m^2 of slab area. It is evident then that the heat loss through an uninsulated slab can be greater than all the remaining conduction heat losses.

EXPERIMENTAL METHODS

Three curing units (30 bulk rack capacity) were built to be installed with a solar energy system. Thermocouples (Type T, ANSI tolerance ± C) were placed under the foundation slabs before the concrete was poured, and in the soil between the units (fig. 2). Units 1 and 3 had 5 cm of polystyrene board insulation (R = 1.5) and Unit 2 had 5 cm of polyurethane board insulation (R = 2.2). The insulation was sealed between two sheets of polyethylene film and the concrete was poured directly on it. Electric resistance blocks (Delmhorst Instrument Company) were used to measure the moisture content in the sand layer, and 20 cm below the soil surface.

A stepping switch scanner (fig. 3) was built as described by Stansell and Cundiff (1976). The copper leads from the thermocouples under the units were connected to the 24 poles of each of four wafers on stepping switch SR2. All of the constantan leads were made common and joined to a copper lead to form a reference junction maintained at 0 C in an ice bath. The thermocouple voltage was amplified (1000 x) and recorded with the minicomputer data acquisition system used for the main solar experiment. The computer was programmed to operate the stepping switch scanner and record the voltage from each thermocouple once each hour. The sequence of operation was as follows. The program recorded thermocouple 1 (pole 1 of wafer 1 on SR2) and then closed a relay on the minicomputer - relay board which shorted SS1 and SS2 to supply + 12 VDC to the coil of relay R1. This relay closed and supplied + 12 VDC to stepping switch SR1 and stepped it to pole 2. SR1 has two wafers, a control wafer and signal wafer with four poles each (fig. 3). The signal wafer has the output from wafers 1 - 4 of SR2 connected to poles 1 - 4 respectively. When SR1 stepped to pole 2, pole 1 of wafer 2 on SR2 was switched into the circuit.

Pole 1 of SR2 wafers 3 and 4 were read as SR1 was stepped by the program to poles 3 and 4 respectively. The control wafer of SR1 was used to charge capacitor C_1 which discharges through the coil of relay R2 and steps SR2 when SR1 steps from pole 4 back to pole 1. This insures proper sequencing of SR1 and SR2. The voltages from the thermocouples connected to pole 2 of the SR2 wafers were then recorded, and the process repeated until all 96 voltages were recorded.

The program converted voltage, V (mV) to temperature, T (C) using the relation

$$T = 25.66V - 6.195 \times 10^{-4}V^2 + 2.218 \times 10^{-8}V^3 - 3.55 \times 10^{-13}V^4 \qquad (1)$$

National Bureau of Standards (1974). The data was then plotted using a digital plotter. Time average temperature over the total cure hours, nh, was calculated for each thermocouple location.

$$\bar{T}_x = \frac{1}{nh} \sum_{j=1}^{nh} T_{xj}$$

ANAYTICAL METHODS

Assuming one dimensional heat flow, the transient temperature profile in a solid is given by

$$\frac{\partial^2 T}{\partial x^2} = \frac{1}{\alpha} \frac{\partial T}{\partial t}$$

where T = temperature (C) (3)

x = distance from surface (m)

t = time (h)

α = thermal diffusivity (m^2/h).

The boundary conditions are

$T = t_o$ at $x \geq o$, $t = o$ (4)

$T = t_x$ at $x = o$, $t > o$ (5)

Here T_o is the ambient soil temperature and is a constant. T_s is the measured temperature function at the surface of the concrete. At any given plane in the profile an energy conservation boundary condition must be satisfied. For example, consider the interface between the ith and (i + 1)th layers,

$$Q_i^{in} = Q_i^{out}, \quad t > o \qquad (6)$$

where Q_i^{in} = heat flux entering the interface between the ith and (i + 1)th layers,

Q_i^{out} = heat flux leaving the interface between the ith and (i + 1)th layers.

As shown in fig. 2 there are four layers of material in the profile under the tobacco curing units, concrete (i = 1), insulation (i = 2), sand (i - 3), and soil (i - 4).

Finite Difference Method

Krieth (1975) gives a finite difference procedure to obtain a numerical solution to Egn. (3). The entire profile composed of the four layers is divided into sublayers of equal thickness Δx. Within the ith layer, the temperature at the center of any sublayer n is given by

$$T(n, t + \Delta t) = \frac{\Delta t\, \alpha_i}{\Delta x^2} \{T(n + 1, t) + T(n - 1, t)\} + \{1 - \frac{2\Delta t \alpha_i}{\Delta x^2}\} T(n, t) \qquad (7)$$

and boundary conditions are rewritten

$$T(n, o) = T_o \qquad (8)$$

$$T(o, t) = T_s \qquad (9)$$

At the interface between the ith and (i + 1)th layers the heat flux out of the interface equals the heat stored in the first sublayer of the (i + 1)th layer plus the heat flux out of the sublayer. Let n denote the first sublayer of the (i + 1)th layer, then the energy balance in equation form is

$$Q_i^{out} = q_n^{out} + \Delta x\, G_{i+1} \frac{\Delta T}{\Delta t} \qquad (10)$$

where q_n^{out} = heat flux leaving the nth sublayer ($MJ/m^2 \cdot h$)

G_{i+1} = heat capacity of the material in the (i + 1)th layer ($MJ/m^3 \cdot C$)

ΔT = temperature change across the nth sublayer during time interval Δt (C).

Using Egn. (6),

$$Q_i^{in} = q_n^{out} + \Delta x G_{i+1} \frac{\Delta T}{\Delta t} \qquad (11)$$

The finite difference form for this equation (Kreith (1975), Schenck (1963)) is,

$$T(n, t + \Delta t) = (k_i (T(n - 1, t) - T(n, t)) - k_{i+1} (T(n,t) - T(n + 1, t)))/\Delta x\, G_{i+1} + T(n, t) \qquad (12)$$

where k_i = thermal conductivity of ith layer (MJ/m · C · h)

Heat Loss Through Concrete Slab

Heat flow through a unit area of the concrete slab during any time interval Δt is given by

$$h = -k_1\ \Delta t(\Delta T/\Delta x). \qquad (13)$$

The gradient, $(\Delta T/\Delta x)$, for each Δt interval is defined by the solution of Egn. (7) with the boundary conditions given by Egns. (8), (9), and (12). Total heat loss was computed by summing the losses for each time interval in the total cure time.

Definition of Effective Diffusivity

Complete information on the thermal properties of the different materials in the profile was not found. The decision was made to use the measured temperature profile to calculate "effective" thermal properties which would yield calculated temperature values equal to the measured values at the interface between the various layers. Gawande (1978) suggests a search procedure which selects a diffisivity value in a given interval which minimizes the following sum of squares,

$$ss = \Sigma_{j=o}^{nh} \quad (T_{xj} - T_{cj})^2, \tag{14}$$

where T_{xj} = measured temperature at bottom of layer at the jth hour,

T_{cj} = calculated temperature at bottom of layer at the jth hour.

His procedure uses the Golden Section Method (Wagner, 1969) to select sucessive diffusivity values.

The effective soil diffusivity (α_4) was determined first. The measured temperature at the top of the soil layer was used for T_s, and T_o was the constant ambient soil temperature measured at a depth of 95 cm. Egn. (7) was used to calculate T_{cj} at a depth of 70 cm and ss was computed using the T_{xj} measured at this point. To find the effective sand diffusivity (α_3), the measured temperature at the top of the sand layer was used for T_s, and T_o was unchanged. Egns. (7) and (12) were used to compute T_{cj} at the bottom of the sand layer, and ss was computed using the T_{xj} measured at this point. The effective insulation diffusivity (α_2) and concrete diffusivity (α_1) were determined in like manner. Conductivity or heat capacity were calculated from the effective diffusivity values by substituting the known value into the relation, $\alpha = k/G$.

RESULTS AND DISCUSSION

The ambient soil temperature measurements showed that the soil temperature was uniform throughout the profile at a given location. An average value of 30 C was used for T_o in the computations. Ambient implies initial soil temperature and temperature at an infinite depth of soil. The temperature measured near the edge of the concrete slab was equal to that measured at the center, within the limits of experimental error. This result verifies the assumption of one dimensional heat flow. All temperatures measured at a given depth were averaged to obtain the experimental temperature ($\bar{T}_x$) at that depth.

The $\bar{T}_x$ values computed at each thermocouple location are given in fig. 5. Note the higher temperatures in the soil under Unit 3 indicating a greater heat flow into this profile, or a higher ambient temperature. The insulation under Unit 2 had the highest thermal resistance, thus, the temperature rise due to heat flow should have been lowest under this unit. In fact the temperature rise was lowest under Unit 1. This may be due to experimental error in the temperature measurement resulting from moisture penetration into the insulation at the point the thermocouples were placed. Care was taken during installation to seal the holes in the polyethylene film which covered the insulation, after the thermocouples were placed. The higher temperatures under Unit 2 probably indicate a reduction in the effectiveness of polyurethane when it is installed as it was here.

The higher temperatures under Unit 3 were due to higher ambient temperatures in this profile. Unit 3 was on the south side of the three unit complex, and the ground beside it was exposed to the sun during the entire day. The experimental test was conducted during August and the sun angle was such that the ground between Units 2 and 3 and Units 1 and 2 were shaded most of the day, as was the ground to the immediate north of Unit 1. Lower ambient temperatures were measured where the ground was shaded. It is possible that lateral heat flow from ambient soil did warm the profile under Unit 3. There was one feature in the construction which did effect lateral flow. Sheet metal covered insulation panels were placed around the edge of the concrete slabs for Units 1 and 2. They covered the lower plenum side wall, the edge of the foundation slab, and extended 20 cm into the soil beneath the concrete. These panels probably reduced lateral heat flow below the slabs and caused the lower ambient temperatures under Units 1 and 2. Comparison of the time average ΔT across the insulation shows that it was 11 C Unit 1 (polystyrene), 10 C Unit 2 (polyurethane) and 9 C Unit 3 (polystyrene). The time average ΔT across the concrete was quite small, only 1 C.

The effective thermal properties of each layer under each unit are given in Table 1. Using a Δx of 0.025 m and a Δt of 0.01 h the temperature profiles under all three units were calculated. A comparison of the measured and calculated profiles under Units 1 - 3 are given in Figs. 4 - 6 respectively. Note that the T_s function is shown on each plot as the temperature profile at the n = 0 sublayer. The maximum observed ΔT across the insulation was 22 C and the maximum across the concrete was 2 C. The values of ss for the various layers indicated the best overall agreement between the measured and calculated profiles for Unit 3 and the poorest agreement for Unit 2.

Heat loss calculated using the effective thermal properties is given in Table 2. Comparison with the heat loss calculated by replacing the insulation with 5 cm of soil shows an energy savings of 21.8 MJ/m^2/cure Unit 1, 24.8 MJ/m^2/cure Unit 2, and 22.0 MJ/m^2/cure Unit 3 resulting from the use of insulation under the concrete slab. The calculated losses with and without insulation were approximately equal for Units 1 and 3 as expected. When compared with Units 1 and 3, the calculated losses for Unit 2 were 9% higher with insulation, and 13% higher without insulation. These results do not indicate an advantage for the higher quality insulation. The calculated losses with insulation do agree with Chang et. al. (1978), 11 as compared to 10 MJ/m^2/cure. Chang et. al. calculated higher losses without insulation, 45.6 as compared to 32.6 MJ/m^2/cure, thus, they report a 40% greater energy savings. The use of the effective thermal properties to calculate heat loss does give a better indication of the benefit derived from the insulation.

SUMMARY AND CONCLUSIONS

Thermocouples were used to measure the temperature profile underneath three tobacco curing structures during a six-day cure. The concrete foundation slab for Units 1 and 3 was insulated from the ground with 5 cm of polystyrene (R =1.5), and Unit 2 had 5 cm of polyurethane (R =2.2). Finite difference techniques were used to calculate temperature profiles for comparison with the measured profiles. The thermal properties of the various layers, concrete, insulation, sand and soil, were adjusted with a search procedure to select those which minimized the sum of squares between the measured and calculated temperature at each layer interface. These "effective" thermal properties were used to calculate heat loss through the concrete slab.

The calculated heat loss was 10.8, 11.9 and 10.6 MJ/m^2/cure for Units 1 - 3 respectively. Without insulation, the calculated heat loss was 32.6, 36.7 and 32.6 MJ/m^2/cure. This indicates an energy savings of 22 MJ/m^2/cure through the use of insulation under the foundation slab of a tobacco curing structure.

REFERENCES

1. ASHRAE. Handbook of Fundamentals. 1974. American Society of Heating, Refrigerating, and Air Conditioning Engineers, Inc., New York, N.Y.
2. Chang, C. S., G. B. Blum, Jr., and W. H. Johnson. 1978. Heat loss through concrete floors of a bulk tobacco curing barn. Tob. Sci. (In Press).
3. Cundiff, J. S. and P. E. Sumner. 1978. Fan cycling and energy savings. University of Georgia Coastal Plain Experiment Station, Agricultural Engineering Department, Tifton, Ga.
4. Gawande, M. 1978. Personal Communication. University of Georgia Coastal Plain Experiment Station, Agricultural Engineering Department, Tifton, Ga.
5. Krieth, F. 1975. Principles of heat transfer. International Textbook Company, Scranton, Pa.
6. National Bureau of Standards. 1974. U.S. Department of Commerce, Washington, D.C.
7. Schenck, H., Jr. 1963. Fortran methods in heat flow. The Ronald Press Company, New York, N.Y.
8. Stansell, J. R. and J. S. Cundiff. 1976. An automatic data collection system for tobacco curing research. ASAE Paper No. 76-3011. ASAE, St. Joseph, Mich.
9. Wagner, H. M. 1969. Principles of operations research. Prentice-Hall, Inc., Englewood Cliffs, N.J.

TABLE 1. Effective thermal properties of various layers under curing structures.

Layer	Diffusivity $m^2/s \times 10^7$	Conductivity $W/m.^{o}C$	Heat Capacity $MJ/m^3 \cdot C$
Concrete	5.794	1.21	2.09[2]
Insulation (polystyrene-Unit 1&3)	29.842	0.104	.035[3]
Insulation (polyurethane-Unit 2)	24.156	0.111	.046[3]
Sand	6.608	1.039	1.270[3]
Soil	7.842	2.903	3.700

1/ Assuming porosity of 50% and moisture content of 50% and using equation presented by Chang et al (1978).

2/ Krieth (1975)

3/ ASHRAE handbook of fundamentals (1974).

TABLE 2. Heat loss through floor with and without insulation for a 140 hour cure.

Unit	Insulation	Heat loss MJ/m^2/cure With Insulation	Heat loss MJ/m^2/cure Without Insulation
L	Polystyrene (sides of concrete slab insulated)	10.8	32.6
2	Polyurethane (sides of concrete slab insulated)	11.9	36.7
3	Polystyrene (sides of concrete slab not insulated)	10.6	32.6

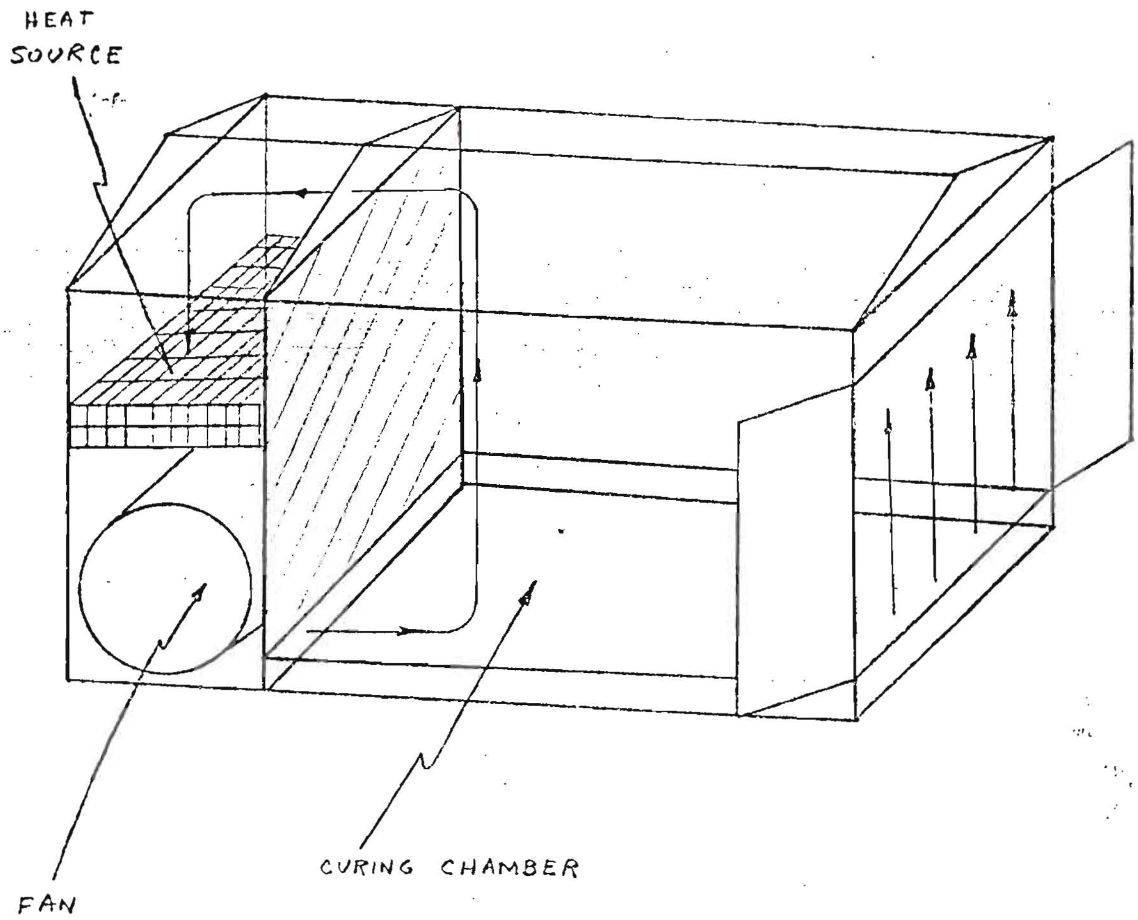

FIG. 1. AIR FLOW IN UPDRAFT BARN
(REVERSED IN DOWNDRAFT)

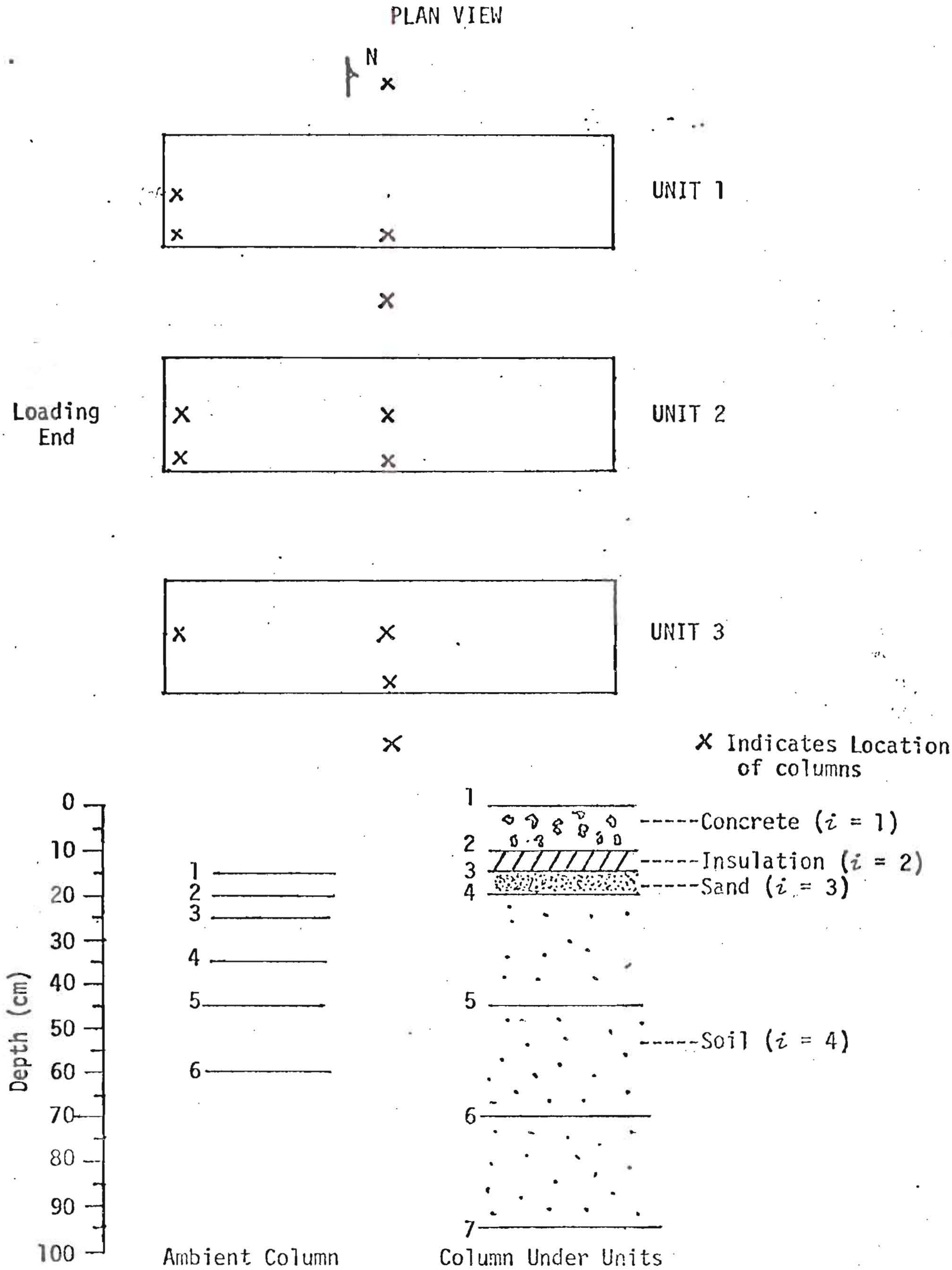

Fig. 2. Location of thermocouples in ambient soil and underneath curing structures.

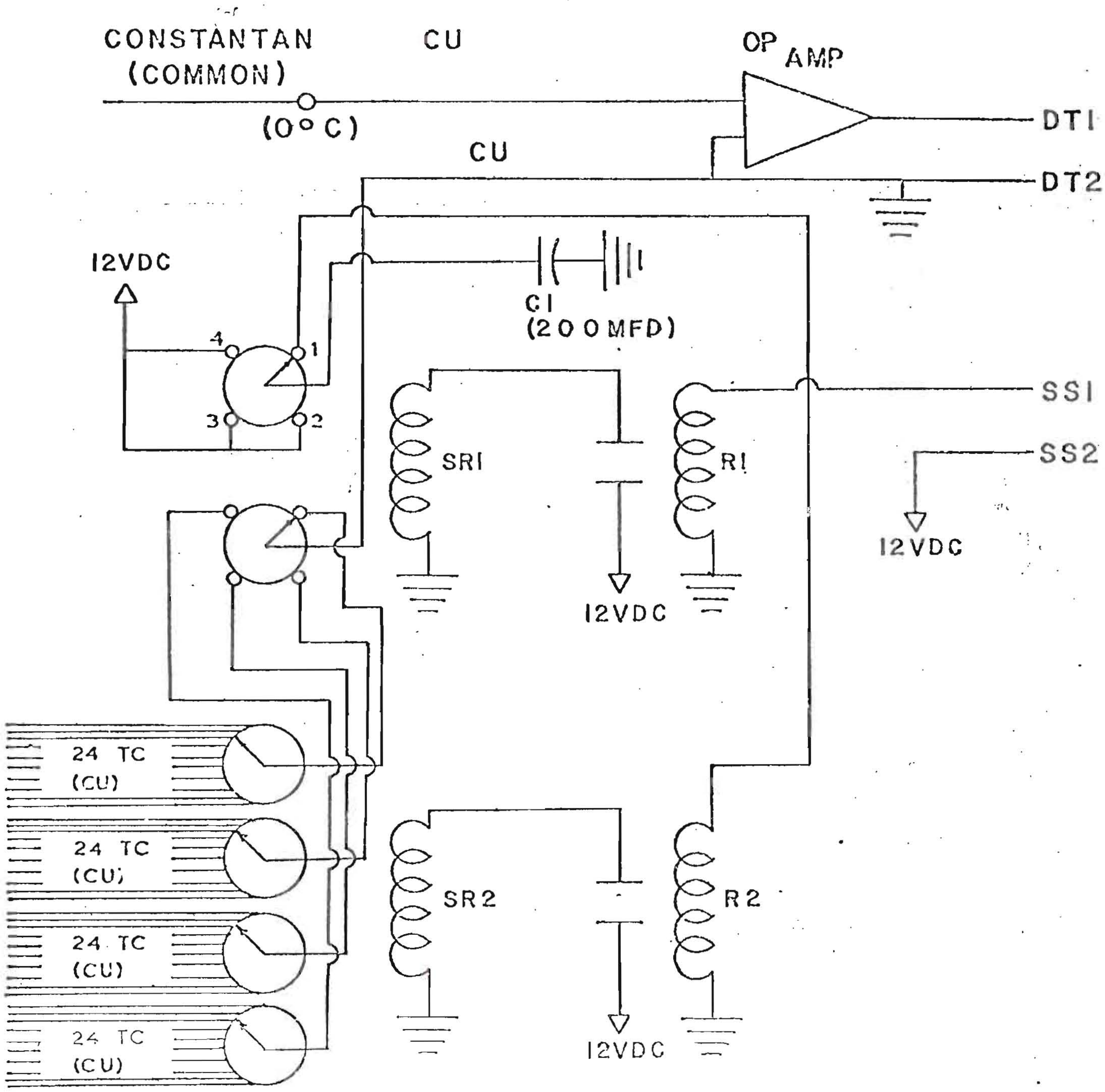

Fig. 3. Stepping switch scanner circuit.

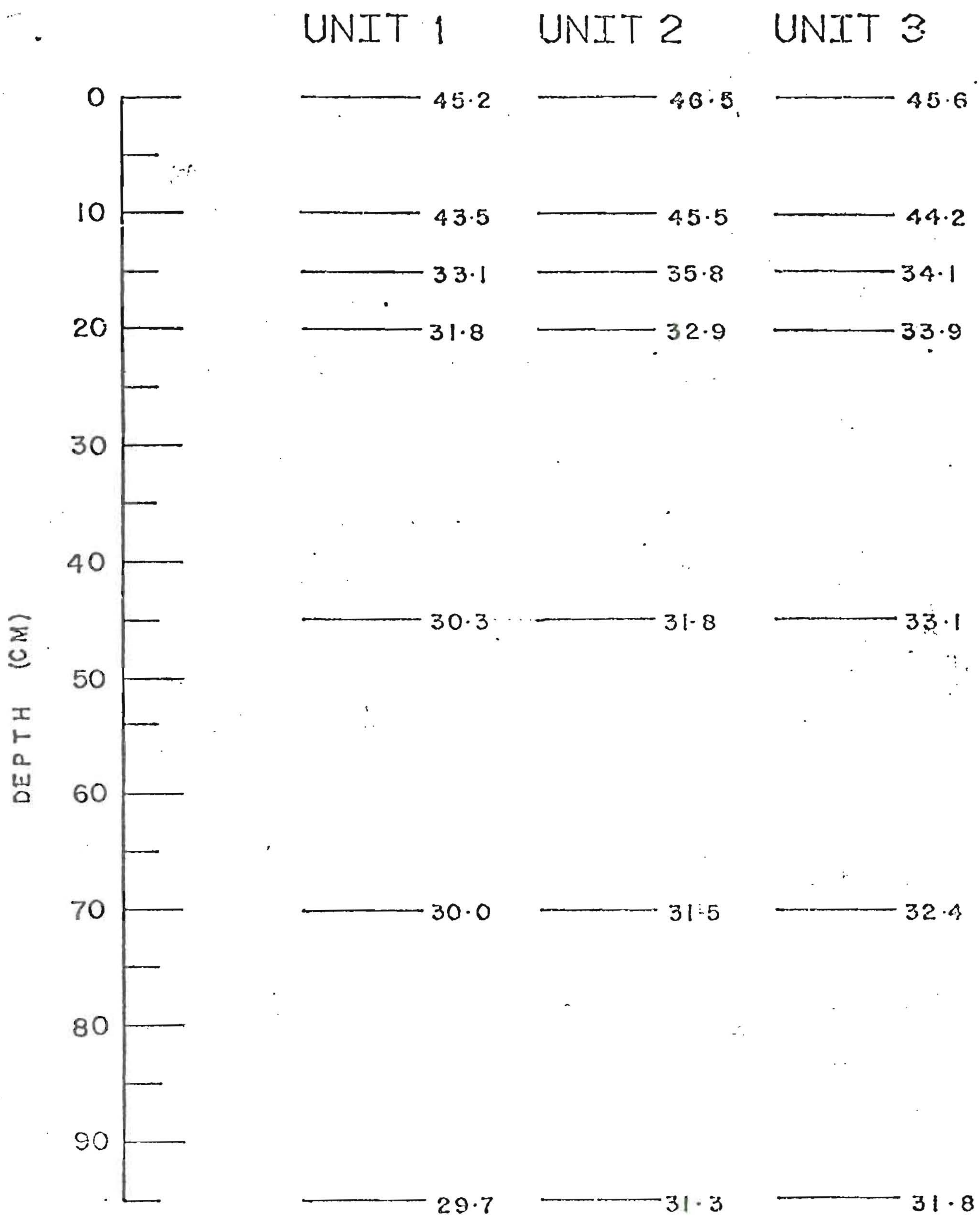

Fig. 4. Time average temperature (C) at various thermocouple locations for six days (140 h) cure.

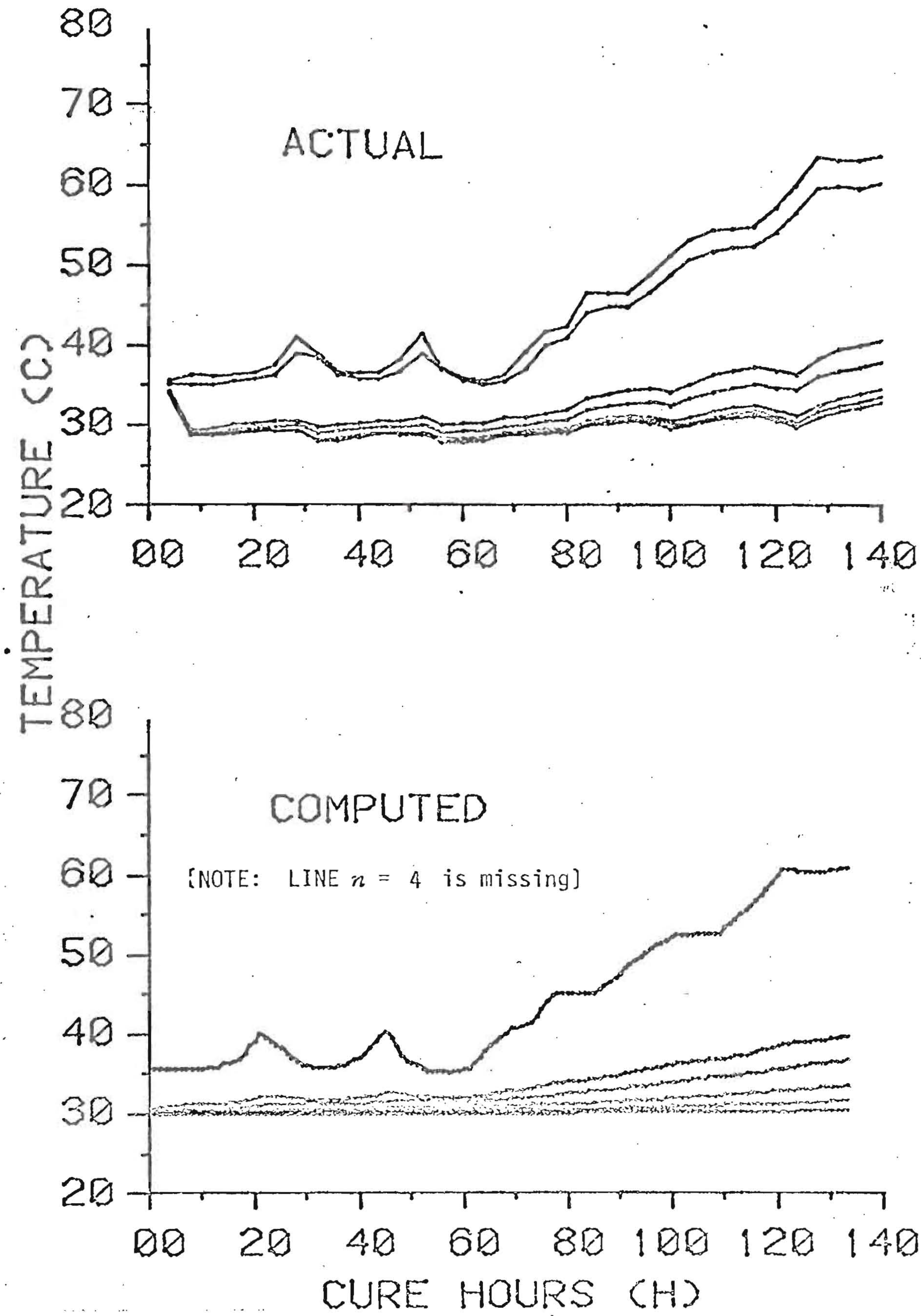

Fig. 5. Measured and calculated temperature profiles under Unit 1.

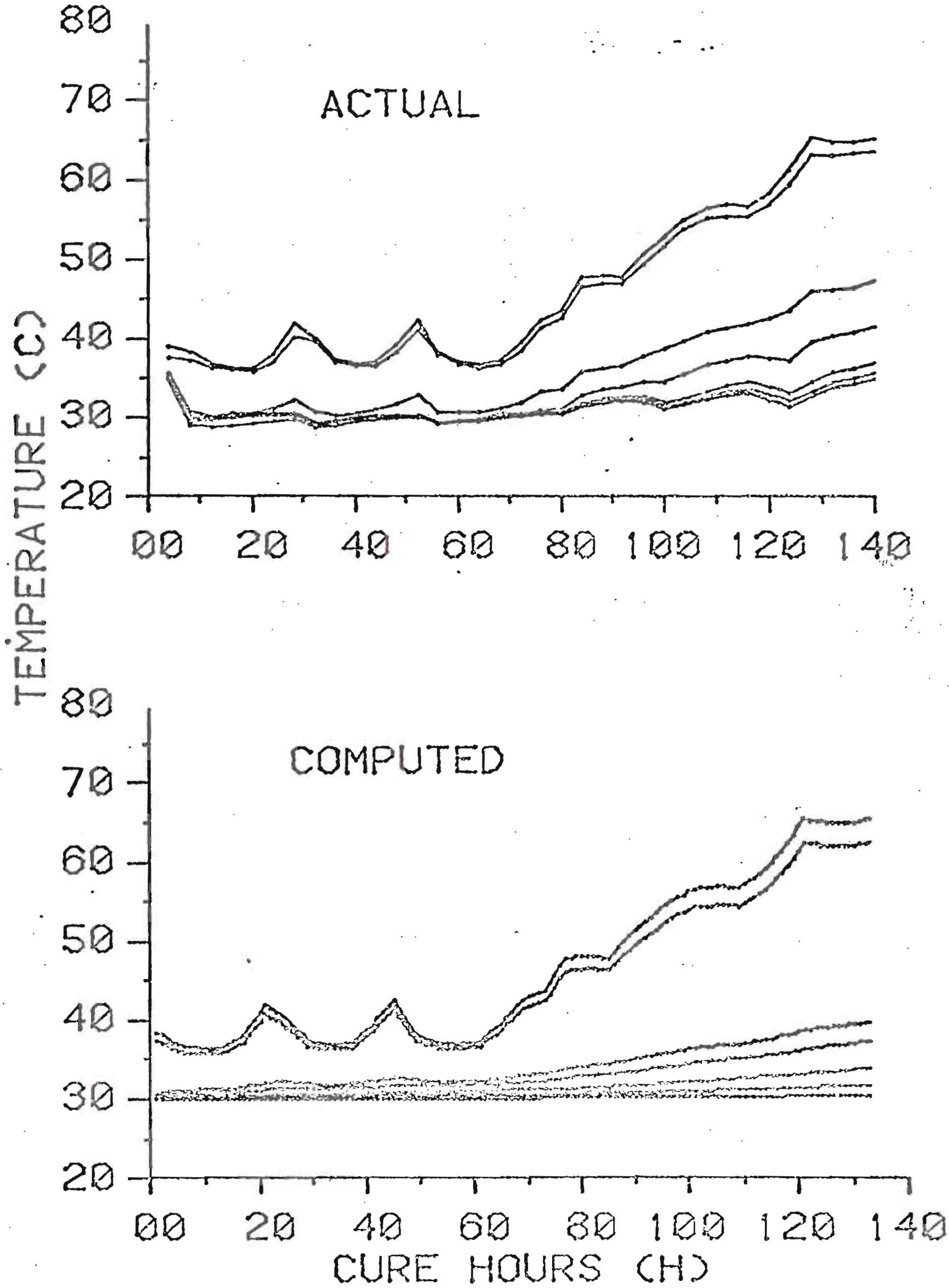

Fig. 6. Measured and calculated temperature profiles under Unit 2.

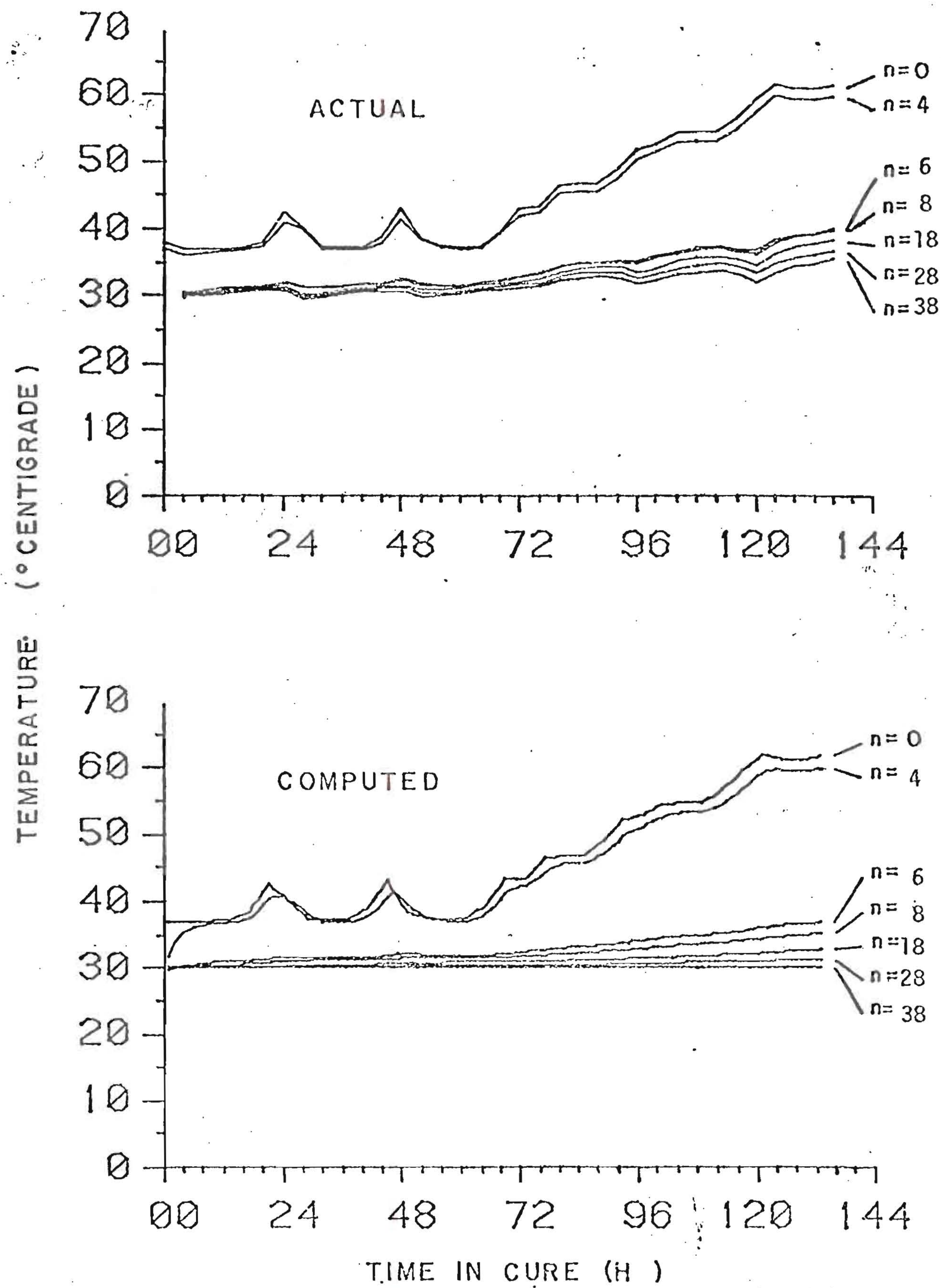

Fig. 7. Measured and calculated temperature profiles under Unit 3.